Bull Volcanol
DOI 10.1007/s00445-010-0373-8

RESEARCH ARTICLE

Deformation structures associated with the Tazo landslide (La Gomera, Canary Islands)

Ramón Casillas · Carlos Fernández · Juan Ramón Colmenero · Julio de la Nuez · Encarnación García-Navarro · M. Candelaria Martín

Received: 1 April 2009 / Accepted: 18 May 2010

Abstract Deformation structures below the basal plane of gravitational slides can provide useful information about the state of stress undergone by rocks prior to the sliding process and about the triggering forces acting at each particular sliding event. In the present work we conducted a structural analysis of the rocks below the surface of the gravitational slide of Tazo (La Gomera, Canary Islands) and determined the epigenetic processes involved in the filling of the amphitheatre. We also inferred the possible triggering phenomena related to the Tazo landslide. The rocks located below the surface of the gravitational slide of Tazo -i.e., the basaltic lava flows, sills and dikes of the Lower Old Edifice and the submarine volcanic rocks, gabbros, pyroxenites and dikes of the Basal Complex of La Gomera- are strongly deformed close to this sliding surface. The lava flows and dikes of the Lower Old Edifice are folded, with fault breccias and gouges, and locally foliated, defining the sliding surface. The dikes of the Basal Complex are also folded, and the gabbros and pyroxenites are affected by a large number of small faults. In the Basal Complex, the sliding surface is defined by a foliated granular gouge. In the damage zone, the Basal Complex rocks show an incipient fracture cleavage. The sliding amphitheatre has been filled by the debris avalanche or cohesive debris flow generated within the slide, as well as by later debris flows, hyperconcentrated flows, sheet flows, and by interspersed lava flows from the Upper Old Edifice. We suggest here that the collapse of the north-western flank of the Lower Old Edifice at Tazo could in part have been triggered by continuous magma injection, associated with the emplacement of dikes in a rift zone with an ENE-WSW direction, enhanced by the mechanical weakness of the Basal Complex unit, which was affected by hydrothermal metamorphism under greenschist facies conditions and by the displacement along the Montaña de Alcalá and Guillama normal faults, which are deeply entrenched in the altered rocks of the Basal Complex.

Keywords La Gomera · Canary Islands · Tazo landslide · Deformation · Debris avalanche · Debris flow

Editorial resposibility: B. van Wyk de Vries.

Electronic supplementary material The online version of this article (doi:10.1007/s00445-010-0373-8) contains supplementary material, which is available to authorized users.

R. Casillas (✉) · J. de la Nuez · M. C. Martín
Departamento de Edafología y Geología, Facultad de Biología,
C/Astrofísico Francisco Sánchez s/n, Universidad de La Laguna,
38206 La Laguna, Santa Cruz de Tenerife, Spain
e-mail: rcasilla@ull.es

C. Fernández · E. García-Navarro
Departamento de Geodinámica y Paleontología,
Facultad de Ciencias Experimentales, Universidad de Huelva,
21071 Huelva, Spain

J. R. Colmenero
Departamento Geología, Facultad de Ciencias,
Universidad de Salamanca,
Plaza de la Merced s/n,
37008 Salamanca, Spain

Introduction

Gravitational landslides on the flanks of large volcanic edifices are one of the most spectacular and catastrophic phenomena that occur at volcanic oceanic islands during their evolution. Many studies have been conducted to analyze the geometry of the scars formed by these landslides, the resulting deposits, and the possible causes of such events. Nevertheless, few studies have analyzed the deformation suffered by the rocks located just below the

Published online: 26 June 2010

main slide plane (Schneider and Fisher 1998; Bachèlery et al. 2003) or the epigenetic/sedimentary processes involved in the filling of landslide amphitheatres. Active volcanoes are unlikely to be suitable for such studies, because even when they are temporarily exposed in fault scarps, the fault rocks themselves are likely to be rapidly buried by lavas, pyroclastic deposits, and volcaniclastic sediments covering the scarps. A more profitable approach may be to study ancient exhumed structures.

In some slide structures on ocean islands, the rocks underneath the slip plane show features indicative of a strong, mostly brittle deformation, such as at La Palma (Roa 2003), with numerous faults and associated secondary fractures, folds, tilted dikes, and shearing of the dike margins, such as the Taganana, Carrizales and Los Gigantes slides in Tenerife (Walter et al. 2005; Walter and Schmincke 2002). The shearing of rocks below the sliding surfaces suggests that creep was active prior to the slide event, causing intense deformation of the rocks involved. Also remarkable is the presence of strong striations under the Toreva or mega-blocks produced by the sliding of these blocks above the slide plane, such as at La Palma (Roa 2003) and Gran Canaria (Mehl and Schmincke 1999).

Deformation studies of rocks below the slide plane can provide useful insights into the stress conditions of rocks prior to the slide process. Such research can help to reveal the ultimate causes of each particular slide event. In this sense, La Gomera island (Canary Islands) provides an interesting opportunity for structural analysis, since the rocks appearing below the slide plane that affected the north-western sector of the Lower Old Edifice -termed the Tazo landslide (Ancochea et al. 2006)- exhibit associated deformation structures. Currently, little is known about the volcanic and sedimentary processes involved in the filling of the scars formed by gravitational flank slides. There appears to be some confusion regarding discrimination between the deposits directly formed by flank sliding (essentially "debris avalanche") and the sediments related to the filling of the slide scars, deposited by gravity flows well after the sliding process (essentially "debris flow") or by running water (essentially hyperconcentrated flows and sheetfloods). The Tazo flank landslide on La Gomera led to the formation of a large landslide amphitheatre that was later filled with sedimentary deposits (polygenetic agglomerates, Cendrero 1971) and numerous basaltic lava flows. The oldest of these basaltic flows are interbedded with sedimentary deposits and form part of the Upper Old Edifice (Ancochea et al. 2006).

The main aim of this work is to describe the deformation structures that appear below the basal plane of the Tazo landslide, and to investigate the deformation mechanisms involved in the slide. Another objective is to describe the amphitheatre deposits in order to explain the volcanic and sedimentary processes involved in the filling of this amphitheatre. A final aim is to deduce the causes of this gravitational slide in light of these data.

Geological setting

The oldest outcropping rocks of La Gomera (Figs. 1 and 2) are the marine sediments, submarine volcanic rocks, plutonic rocks and dikes forming the Basal Complex (Bravo 1964; Cendrero 1971). The submarine volcanic rocks outcrop in the north-western sector of the island and are constituted by basaltic pillow lavas, peperites, breccias, volcanic sandstones and siltstones, and trachytic breccias of unknown age (Cendrero 1971; Casillas et al. 2008a). Subvertical layers of marine sediments of unknown age (sandstones, limestones, cherts and carbonate layers) are related to these submarine rocks (Cendrero 1971). A suite of plutonic rock bodies, dated at between 19.8 and 7.5 Ma, appears in the Basal Complex (Abdel-Monem et al. 1971; Cantagrel et al. 1984; Herrera et al. 2008). Taking into account the spatial relationships of the plutonic rocks and the effects of contact metamorphism, they can be grouped within three plutonic events of different ages (Cendrero 1971; Démeny et al. 2010), a) hornblende pyroxenites (with kaersutite as the dominant amphibole), hornblendites (with kaersutite as the dominant amphibole), and amphibole gabbros (P1); b) wehrlites, clinopyroxenites, olivine gabbros and gabbros (P2) and c) alkaline gabbros, monzodiorites and syenites (P3, Tamargada Complex). An important dike swarm intrudes these sedimentary, volcanic and plutonic rocks (Cendrero 1971). This dike swarm is characterized by a high dike density and compositional variety, in spite of its dominant N70°–80° strike. All the rocks of the Basal Complex are strongly faulted (Cendrero 1971) and have been affected by a strong hydrothermal metamorphism in greenschist conditions that led to the formation of hornblende, actinolite, epidote, albite and chlorite.

La Gomera island began to emerge around 10.5 Ma ago with the formation of the Old Edifice (formed between 10.5 and 6.4 Ma), with shallow submarine rocks at the base (Ancochea et al. 2006). Two stages of growth of the Old Edifice have been distinguished. In the first stage, a large basaltic shield edifice was formed (Lower Old Edifice), with a diameter of 22 km (Ancochea et al. 2006). This edifice underwent several flank slide events (e.g. Tazo and San Marcos) that dismantled a large portion of its northern sector (Paris et al. 2005; Ancochea et al. 2006). In the second stage of growth (Upper Old Edifice), the activity migrated to the south and a wide composite volcano with a diameter of 25 km was developed, covering the rocks of the Lower Old Edifice. Finally, a young volcanic edifice grew (Young Shield Edifice) between 5.7 and 4 Ma ago

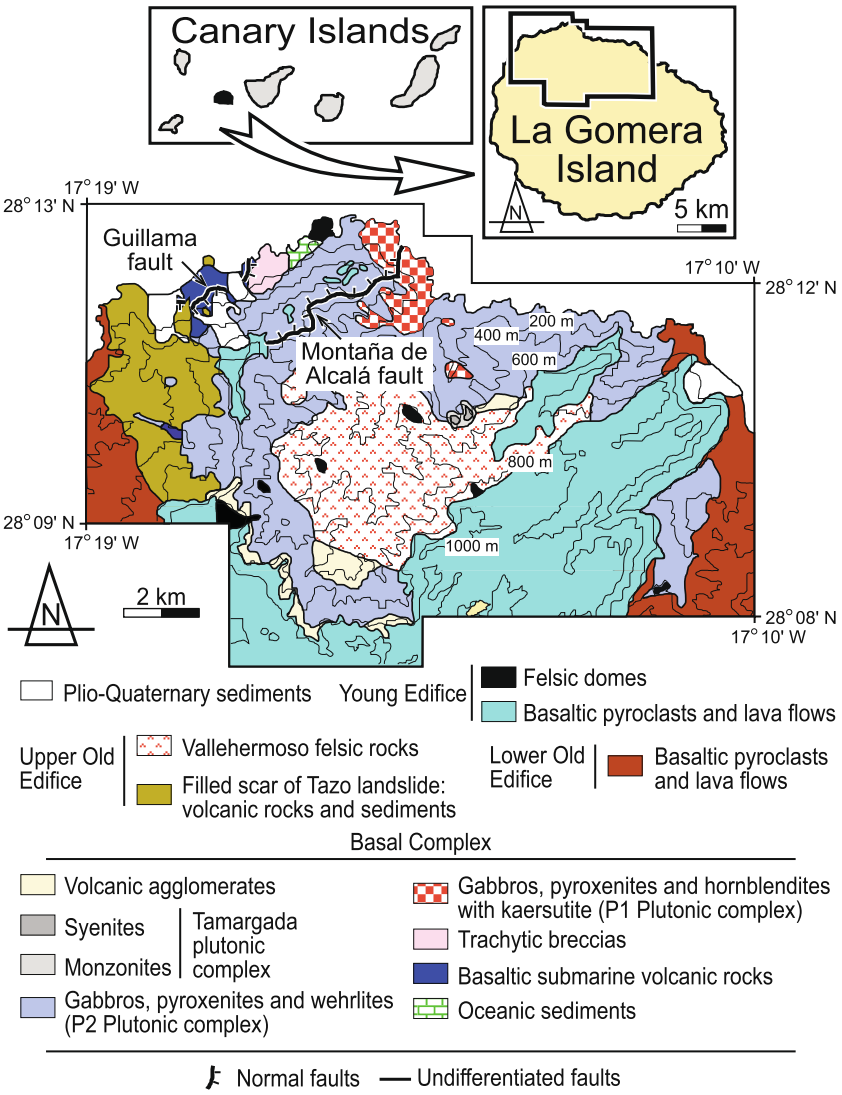

Fig. 1 Geologic map of the northern sector of La Gomera. The map is based on data from Cueto et al. (2004a, b), as modified by us. The inset shows the location of La Gomera in the Canary Archipelago and the area covered by map

(Ancochea et al. 2006). The lava flows of this edifice covered the central and southern parts of the island completely, filling up deep valleys in the north.

The Tazo landslide

General description

The Tazo landslide (Figs. 1, 2 and 3a) occurs in the northwestern sector of La Gomera and it affected the northwestern flank of the Lower Old Edifice. The age of the sliding has been dated at about 9.4 Ma (Ancochea et al. 2006). The flank landslide left a large scar that was filled up with debris avalanche, debris flow, hyperconcentrated flow, and sheetflood deposits corresponding to the polygenetic agglomerates of Cendrero (1971). At the same time, volcanic activity was reinitiated, giving rise to numerous basaltic flows that formed the Upper Old Edifice (Ancochea et al. 2006). The oldest of these basaltic flows are interbedded with the sedimentary deposits filling the slide scar (Herrera 2008).

The basal plane of the Tazo slide outcrops extensively in the Tazo-Alojera-Argüamul-Guillama sector. Towards the Northeast (Arguamul-Guillama) and to the South (Tazo), the rocks of the Basal Complex outcrop below the plane. These are submarine volcanic rocks, gabbros and pyroxenites, intensely intruded by dikes of varying composition. Northwestwards (Alojera-Bejira), the basaltic flows of the Lower Old Edifice appear below the sliding surface, dipping towards the northwest, and they are intruded by sills and vertical dikes of the same composition. The slip plane is truncated by the present-day coastline (Fig. 2) and has been eroded by wave action and by the frequent Quaternary coastal slides that have occurred in this sector, such as that of Arguamul (Paris et al. 2005). Inland, the slip plane is overlain by the horizontal lava flows of the Young Shield Edifice

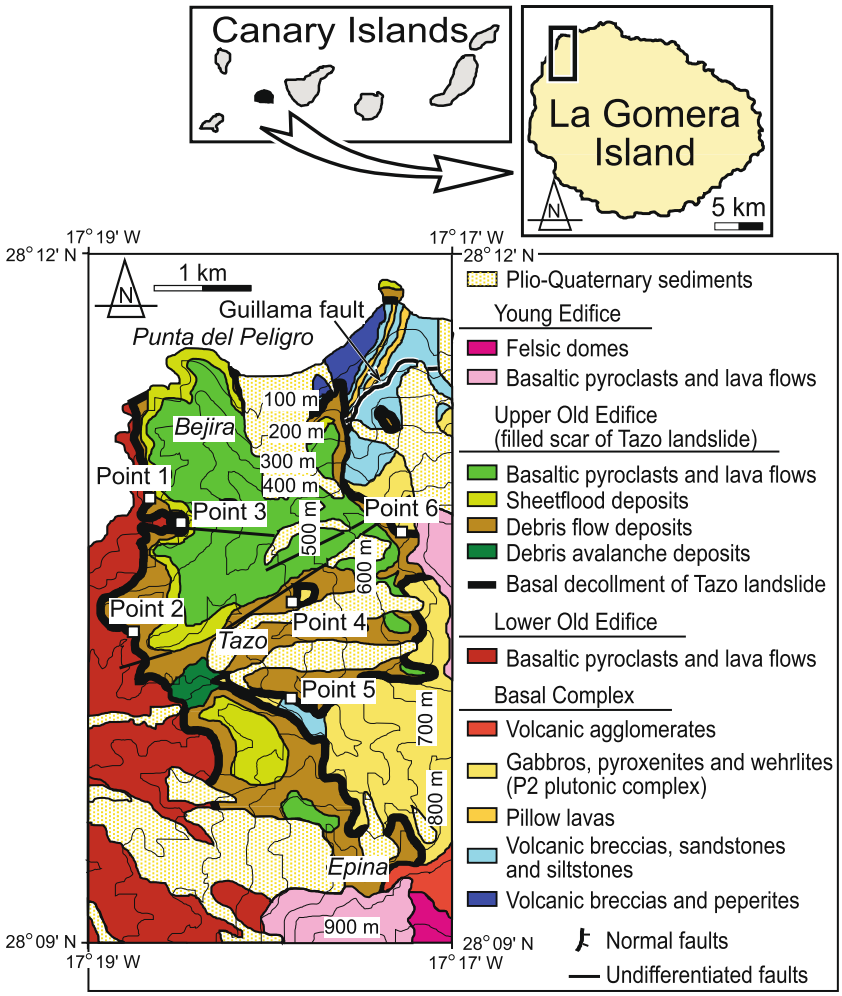

Fig. 2 Detailed geologic map of the Tazo landslide. The map is based on data from Cueto et al. (2004a, b), as modified by us. The inset shows the location of La Gomera in the Canary Archipelago and the area covered by map

(Fig. 3a). The highest altitude of the sliding surface outcrops is 830 meters, at Epina (Fig. 3a).

Structures associated with the Tazo landslide

On the coast, between La Punta del Peligro and La Baja del Picacho, large cliffs expose a major contact, defined by a continuous and regular surface dipping 20° towards the north (Point 1 in Figs. 2 and 3a). This major contact will be referred to as "contact surface" throughout this section of the structural description. A volcanic breccia can be observed above the contact surface, and curved lava flows, sills and dikes of the Lower Old Edifice lie below it (Fig. 3b). Trachyphonolitic dikes of the radial dike complex (Ancochea et al. 2006) associated with the Vallehermoso felsic rocks (Fig. 1) and some undeformed basaltic dikes cross-cut the contact plane, which has been displaced by normal faults dipping towards the southwest.

The same contact surface is visible near the small village of Cubaba (Point 2 in Fig. 2), where it is possible to observe the deformation that has affected the dikes and lava flows of the Lower Old Edifice in detail (Fig. 4). Around 100 m below the contact surface, the Lower Old Edifice is composed of 1-m-thick flows of basaltic pahoehoe lava. Thin sills and E-W oriented, subvertical, less than 1-m-thick basaltic dikes, with an average spacing of 10–15 m, have intruded the lava flows. These rocks do not show evidence of deformation. At around 15 m below the contact surface, the lava flows and sills are cross-cut by subvertical cracks infilled by highly cemented breccias formed by subangular and heterogranular fragments of lava flows and basaltic dikes, with diameters of up to 5 cm (Fig. 4a). These infilled cracks are typically between 0.5 and 5 m thick and are WNW-ESE oriented. The widest ones have a wedged geometry and are infilled by a breccia similar to the one located above the major contact surface. At around 10 m below the contact surface the basaltic flows and sills are thinned and stretched and appear completely broken and brecciated, although their edges are still recognizable. They are overturned and form folds (Figs. 4b and 5a, b). The spatial orientation of the sill walls and lithological layering (S_0) separating the distinct lava flows has been measured in the field and is projected (great circles) in Fig. 5a. If measurements were made without error and the fold was

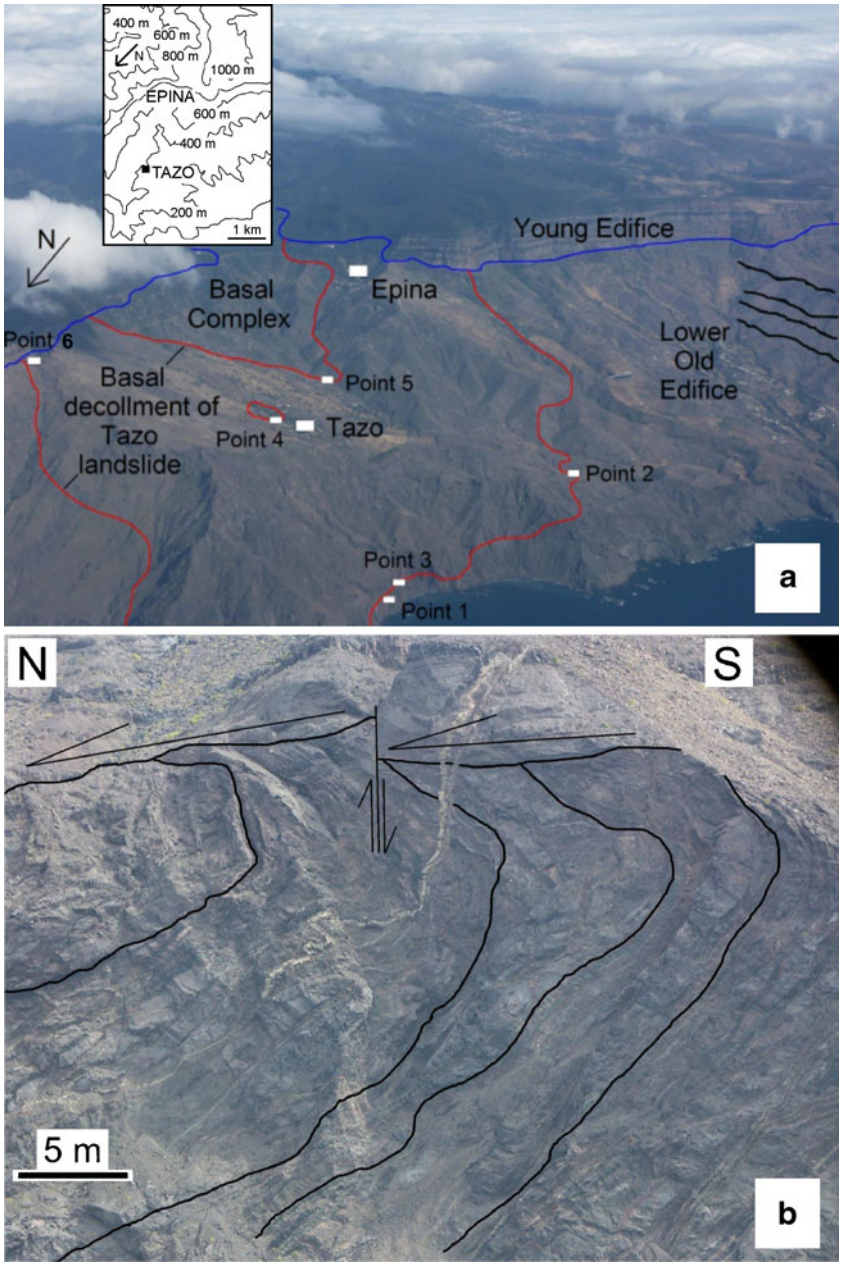

Fig. 3 **a**) Aerial image (view from northwest) of the Tazo landslide. **b**) Interpreted photograph of the sliding surface of the Tazo landslide on the coastline at Point 1

perfectly cylindrical all the great circles would pass through the same axis, which coincides with the fold axis (Ramsay and Huber 1987). However, these conditions are rarely, if ever, met (see Fig. 5a). Fold axes can be determined with maximum accuracy by finding a best-fit great circle for the poles of the measured data, the perpendicular to this great circle lying parallel to the fold axis (Ramsay and Huber 1987). A standard statistical procedure to determine the best-fit great circle and its normal line is to compute the eigenvectors of the matrix that expresses the moment of inertia of the poles to the measured data in a given direction (Mardia 1972). The eigenvector associated with the maximum moment of inertia represents the line most normal to all the measured poles as possible, thus representing the statistically determined fold axis. A confidence level can be assigned to the results of this procedure. The statistically determined axes of the folds measured at Point 2, for both S_o and the sill walls, plunge slightly to the north (Fig. 5a) and are sub-parallel to the main contact surface. The fold geometry can best be described as a progressive rotation of lava flows and sills from a regional, northwest-dipping attitude towards a position parallel to the contact surface (large arrow in Fig. 5a).

Around 4 m below the contact surface, the lava flows and sills are very deformed. It is possible to observe individual sills and lava flows that have become progressively reoriented, stretched and brecciated while

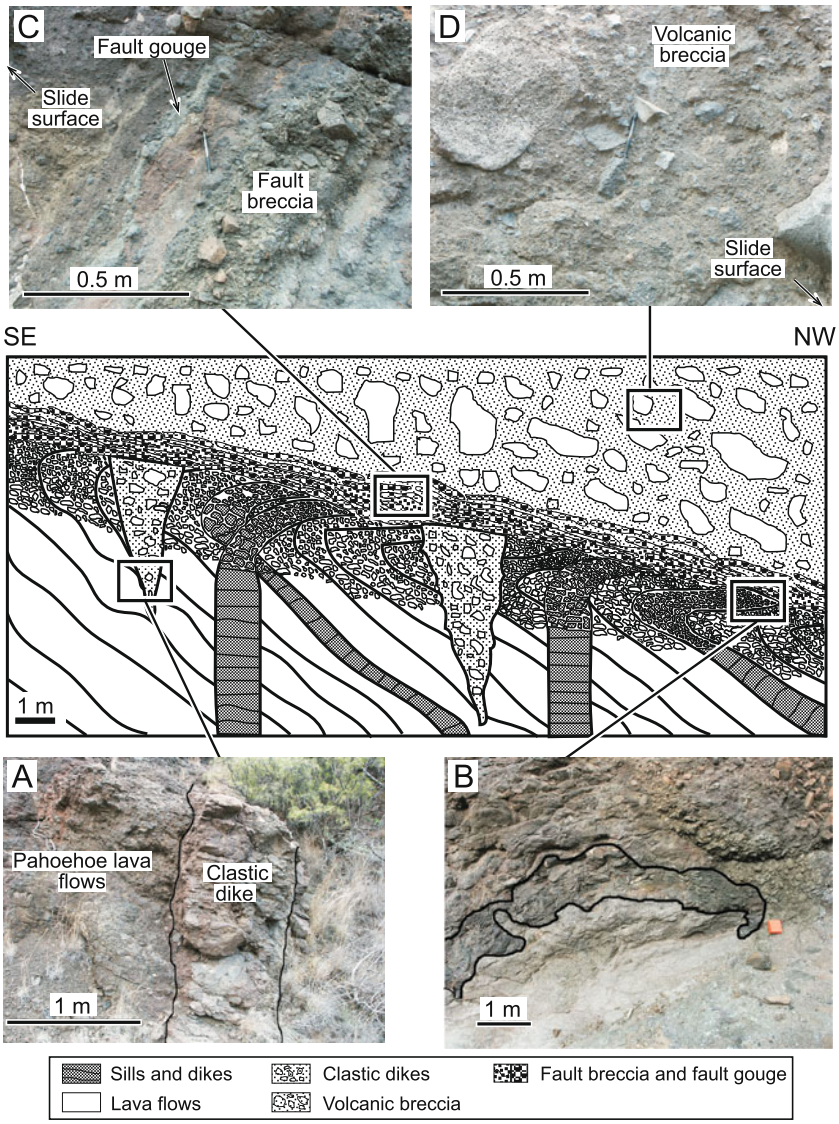

Fig. 4 Deformation structures and rocks related to the displacement along the contact (slide) surface between the volcanic breccias and their substratum at the outcrop near the village of Cubaba (Point 2 in Fig. 2). **a**) Interpreted photograph of an E-W-oriented infilled crack (clastic dike). **b**) Interpreted photograph of a folded sill. **c**) Photograph of the fault breccias and fault granular gouges below the contact surface. **d**) Photograph of the volcanic breccia located above the contact surface

approaching the contact surface, forming a fault breccia (Fig. 4b) composed of very angular fragments of up to 2–5 cm in diameter without matrix. There are cracked grains (jigsaw fit); –i.e. angular fragments that have been fractured without much displacement, such that the original spatial relationships of the fragments can still be recognized. The fragments, which are very angular, do not appear to have been rotated. Here the sub-vertical dikes show a curved geometry, reaching a sub-horizontal orientation a few meters below the slide plane. Moreover, they display a fragmented pattern similar to that of the lavas and sills. At only 1 m below the contact surface, the dikes and the lava flows are crushed, and the fragments of each unit define thinned and stretched bands, following planes that are parallel to the slide surface and forming foliated breccias (Fig. 4c). Closer to the contact surface, the stretched bands give rise to a foliated granular gouge. In this zone, it is frequently possible to recognize the different lava flows and dikes, in spite of the intense fracturing, with fragments of up to 10–15 cm included in a fine-grained cataclastic matrix. The fragments may have undergone a small rotation. Above the contact plane, a poorly sorted, unstratified and structureless**,** highly heterogranular and heterolithologic breccia occurs. It contains subangular fragments of lava flows and dikes of up to 1 m in maximum diameter (Fig. 4d). The matrix of this breccia is composed of angular fragments of volcanic rocks, dikes, and plutonic rocks, with highly heterometric grain-size populations, ranging from fine gravel to clay.

In the La Barca Valley (Point 3 in Fig. 2), the foliated-to-granular gouge located immediately below the contact plane often displays fragment mixing, abrupt changes in unit thickness, folding, flow structures, and other signs of mesoscopic ductility (Miller 1996). Microscopically, this gouge contains survivor grains (between 0.2 and 5 mm) composed of basaltic fragments, typically rounded to sub-

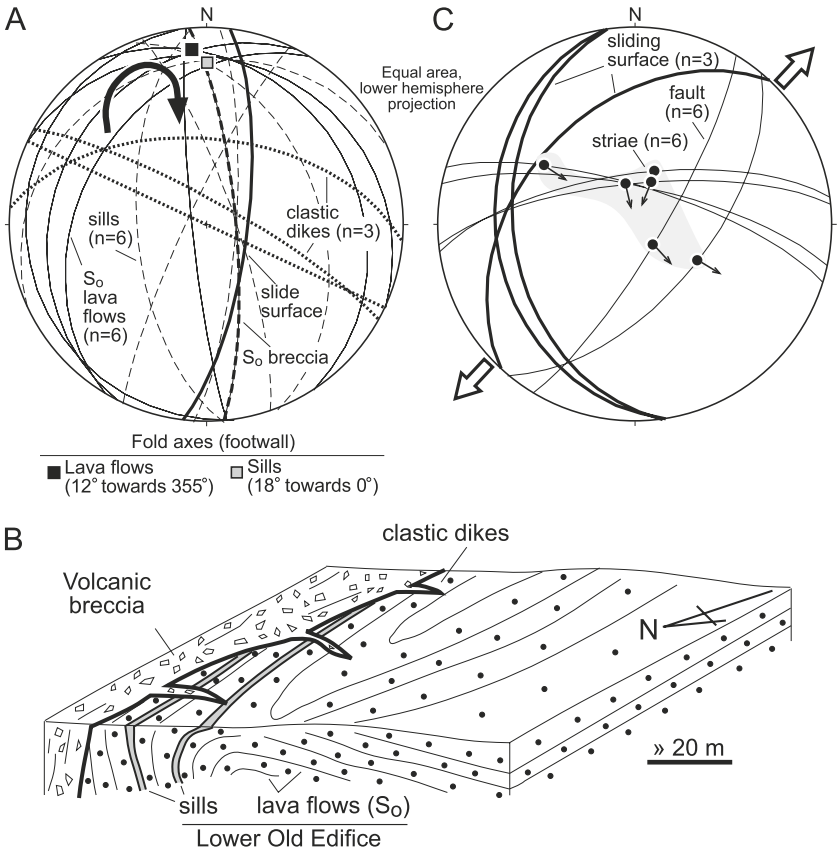

Fig. 5 **a**) Structural data relative to Point 2. Equal-area, lower-hemisphere projection of layering (S_o, lava flows of the Lower Old Edifice below the contact surface and the breccia above the contact surface), sills, infilled cracks (clastic dikes) and contact surface (sliding surface). The squares mark the location of the statistical fold axes for the folded lava flows and sills (see main text for an explanation of the methodology used to determine fold axes). The confidence level of the fold axis determination is >99% for the S_o of lava flows and in the range of 90–95% for sills. The large black arrow indicates the rotation of the lava flows and dikes towards a position parallel to the sliding surface. **b**) Sketch depicting the geometry of the deformation structures associated with the contact surface at Point 2. **c**) Structural data measured at Point 4 projected on equal-area, lower-hemisphere diagrams. Cyclographic projection of the contact surface and of late reverse and normal faults. The large white arrows indicate the sliding direction according to the fault-slip data (see Supplementary Material). In all cases, (n) indicates the number of measured data

rounded and showing little evidence of fracturing, crystal-plastic deformation, dissolution, or mineral growth. The survivor grains are floating in a foliated or banded matrix composed of clay minerals and/or extremely fine grained (<0.01 mm) remnants of the parent rock, plagioclase, and pyroxene crystals.

Near Tazo (Point 4 in Fig. 2), dike-injected gabbros and pyroxenites of the Basal Complex are present below the contact surface. This surface trends NNW-SSE to NE-SW and dips slightly to the West (Fig. 5c). As at Point 1, the plutonic rocks and dikes are strongly deformed around 20 m below the contact surface. These deformed rocks display numerous closely-spaced small faults that define a fracture cleavage. The breccia located in the hanging wall of the contact surface is also faulted near its basal contact. The slickenside features of these faults are indicative of the slip motion along the main contact surface. These faults were analyzed with the kinematic PT method of Marrett and Allmendinger (1990) to obtain the orientation of the principal deformation axes (the results of the PT method for the different measurement points are shown in Supplementary Material). The faults measured are predominantly normal and hence the maximum shortening (P axis) is almost vertical. The principal extension (T axis) is sub-horizontal and trends N43°E (Fig. 5c). In the most severely deformed zone, immediately below the contact surface, a foliated granular gouge with an average thickness of about 20 cm and very angular fragments can also be observed (Fig. 6a). Beneath this gouge layer, there is a fault breccia with angular fragments of dikes and plutonic rocks showing polished and striated facets. In the foliated granular gouge, the larger fragments (up to 5 cm) seem to have been rotated and are considered survivor grains (Cladouhos 1999). Sometimes the foliated granular gouge displays evidence of mobilization because it has infilled small cracks that cut across the contact surface and the overlying deposits of the volcanic breccia (Fig. 6b). Above the contact surface, a volcanic breccia showing sharp contacts can be observed,

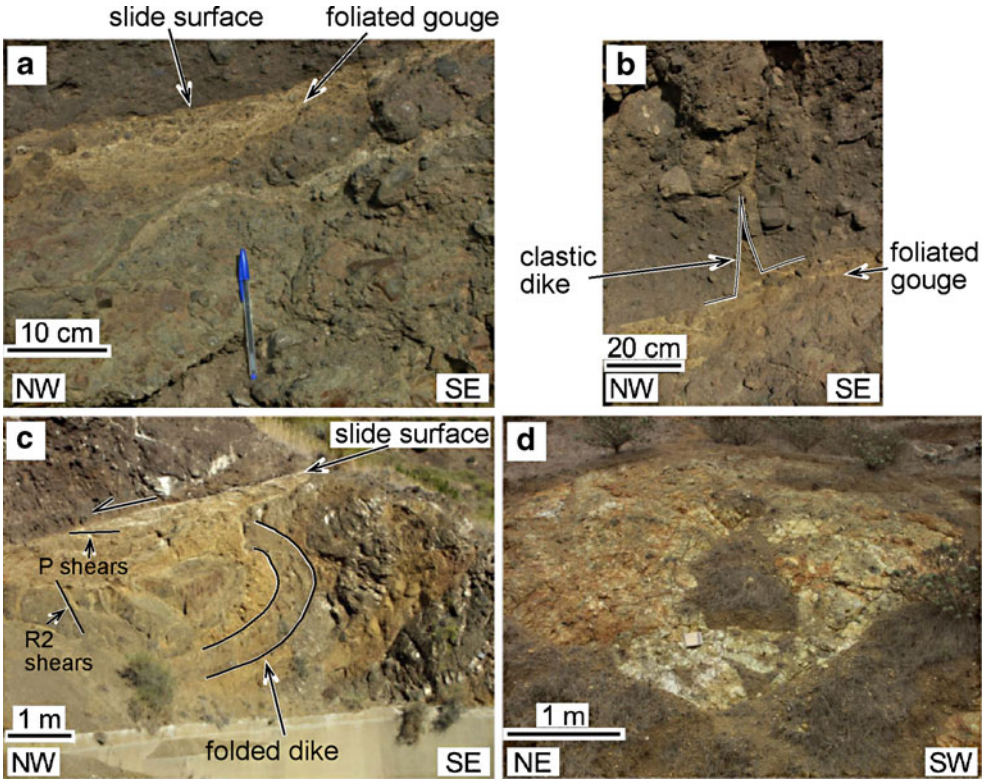

Fig. 6 Photographs of the structures associated with the landslide near Tazo (Points 4, 5 and 6 in Fig. 2). **a**) Photograph of the foliated fault breccia and foliated granular gouge below the contact (sliding) surface. Note the volcanic breccia above the slip plane. **b**) Foliated gouge intruding the volcanic breccia along a fracture, forming a clastic dike. **c**) Photograph of the contact surface at Point 5. Folded dikes, P fractures, and Riedel R2 surfaces below the contact surface can be observed at this point. **d**) Photograph of the striated ultra-fine gouge at the contact surface at Point 6

whose sedimentary features are similar to those of the volcanic breccia overlying the contact surface at Point 2. The contact surface is frequently affected by later E-W- to NE-SW-trending normal and reverse faults (Fig. 5c), which points to late NW-SE directed displacements.

Near Tazo (Point 5 in Fig. 2), the contact surface is E-W-trending and dips slightly to the North (Figs. 6c and 7a). Above the contact surface there is a volcanic breccia overlying an ultrafine-grained gouge (particles <62.5 μm) composed of angular fragments of volcanic and plutonic rocks. This gouge layer, in which ENE-WSW-trending striae can be observed (Fig. 7a), shows an average thickness of about 2 cm. The striae and associated steps indicate the direction of motion along the contact surface (top towards the ENE, small arrows in Fig. 7a). The PT method reveals a N56°E-trending principal extension for these predominantly normal faults (large open arrows in Fig. 7a). This estimated direction of extension is compatible with the small-scale kinematic indicators along the contact surface described above. Beneath the contact surface, the dikes intruding the gabbros are folded (Fig. 6c). The statistical fold axis plunges 14° towards N75°E (Fig. 7a) and is almost parallel to the extension and sliding direction along the main contact surface. Far away from the major contact, the dikes dip at high angles to the SE and show a curved geometry below the contact surface, tending to become parallel with that surface (large curved arrow in Fig. 7a).

On the road from Tazo to Montaña de Alcalá (Point 6 in Fig. 2), the contact surface shows steep dips to the WNW (Fig. 7b). The faults located in the close vicinity of this contact are sub-parallel to it and their slickenside features show that they are normal faults with hanging wall blocks exhibiting westward, down-thrown motions (old striae in Fig. 7b). However, in some cases it is possible to observe a second set of striae that partially erases the previous set and indicates a late strike-slip reactivation of the contact surface. The layer of ultrafine-grained gouge located at the contact surface can be seen in Fig. 6d. A fault measurement station was set up at the breccias located above the contact surface at this point. The results of the PT method show that the principal direction of extension is sub-horizontal and trends N21°E; i.e. intermediate between the old and new kinematic indicators observed along the contact surface (Fig. 7b, large white arrows).

Sedimentological features of the rocks infilling the flank-collapse amphitheatre

The epiclastic deposits that partially infill the Tazo landslide depression outcrop markedly at the Santa Catalina beach and the adjacent Punta del Peligro cliffs. As in other giant landslides found in the Canary Islands, the infilling sequence of the Tazo slide scarp involved two successive unconformity-bound units with different textural features, sedimentary structures, and origins (a stratigraphic section is shown in Supplementary Material).

The lower unit ranges from 10 to 20 m in thickness. It consists of chaotic, poorly to extremely poorly sorted,

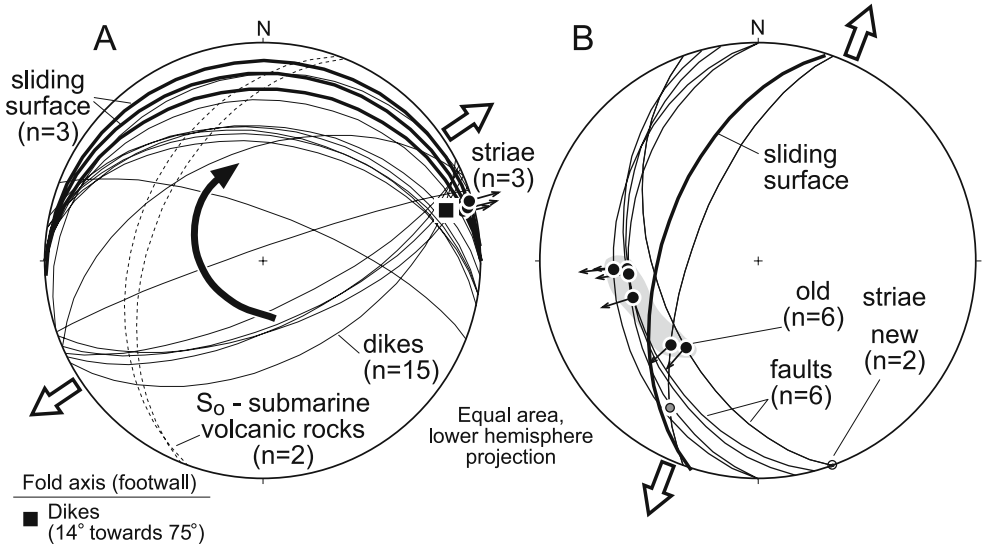

Fig. 7 **a**) Equal-area, lower-hemisphere plot of the structural data measured at Point 5. Contact (sliding) surface with slickenside striations marking the sliding direction, and attitude of lava flows of the submarine volcanic rocks (footwall of the sliding surface). The large white arrows indicate the location of the principal extension axis, according to the results of the PT method (see Supplementary Material). Also shown is the cyclographic projection of folded dikes located at the footwall of the contact surface with the location of the statistical fold axis. See main text for an explanation of the methodology used to determine fold axis. The confidence level of the fold axis determination is >99%. The large black arrow highlights the progressive rotation of the dikes towards a position parallel to the contact surface. **b**) Equal-area, lower-hemisphere plots of the structural data measured at Point 6. Contact surface and faults located in the vicinity of the contact surface and sub-parallel to it. The faults show two generations of slickenside striations (old and new). The large white arrows indicate the location of the principal extension, according to the results of the PT method (see Supplementary Material)

matrix-supported, boulder-to-pebble-sized breccias. The clasts mainly consist of basaltic dikes and lavas, although there are also fragments of gabbros and pyroxenites. They are angular to subangular, up to 2 m size, and they do not show any preferential orientation. The matrix is a mixture of sand and fine pebble-sized particles with the same composition as the clasts. The unit has a massive appearance, although a crude inverse grading can be observed at the base. A large stratified block formed by a sequence of ropy basaltic lavas (roughly 50 m thick) and scattered, metre-scale blocks with a jigsaw-fit structure are also present towards the lower part of the unit. This unit represents the first stage of the slide scarp fill after its lateral gravitational collapse.

The upper unit reaches some 100 m in thickness and displays a greater lateral extension than the underlying one. The boundary between both is a sharp and irregular erosive surface. The bulk of this unit is made of moderately-to-poorly sorted, slightly bouldery, pebble-to-cobble clast-supported conglomerates in decimetre- to-metre scale beds, which are crudely interstratified with fine-to-medium pebble gravel and subordinate coarse pebbly sandstones. The clasts vary from subangular to rounded and mainly lie parallel to the bedding, although an a-axis imbrication of the elongate clasts is also present. The bed geometries vary from irregular to lenticular, with sharp and slightly erosive bases, to laterally continuous at outcrop scale. Planar and trough medium-scale cross-strata are commonly visible throughout the unit in the pebble and sandstone intervals. Coarse boulders are found widely dispersed as outsized clasts or concentrated in scours that may reach 1 m in depth. Some beds also display a reverse-to-normal grading. Large-scale planar cross-bedding with inclined laminae displaying a sigmoid shape present at the lower part of the unit is thought to represent frontal or lateral accretion units of macroforms within alluvial channels. There are frequent interbedded basaltic lavas.

Discussion

Interpretation of the structures observed: the slide surface of the Tazo landslide

The major contact defined in the structural description systematically separates the volcanic breccias infilling the Tazo slide amphitheatre at its top, and variably deformed rocks of the Basal Complex and Lower Old Edifice at its base. A deformation gradient can be observed below the contact surface, with the most intensely deformed rocks located immediately below and along that surface. These features, together with the large spatial continuity of the contact surface across the area studied (Fig. 2), lead us to propose that it would correspond to the main slip surface of

the Tazo slide. In some sectors of the Tazo slide (Points 5 and 6), the base of the volcanic breccia is formed by an ultrafine-grained gouge, which forms a band of around 2 cm in thickness. NW-oriented striae are observed locally in this band, indicating the slip direction. The microscopic characteristics of this gouge suggest that the survivor grains can be treated as rigid clasts in a viscous flow. A gravitational flank landslide of a volcanic edifice can be considered a low-angle normal fault in which the footwall remains immobile and the hanging wall moves along the fault plane, either as a single block (translational sliding) or as a block that becomes disintegrated during its movement due to the progressive fracturing, disaggregation, and mixing that occur during the flow, leading to the formation of a rock slide debris avalanche. Thus, as in a normal fault, the elements of the footwall exhibit deformation due to the relative movement of the hanging wall. Indeed, in the gravitational landslide of Tazo, the underlying rocks below the slip surface underwent a significant degree of deformation: the folding of lava flows and dikes due to the dragging effect of the sliding block, the fracturing of lava flows, plutonic rocks and dikes whose fragments form bands parallel to the movement surface, giving rise to fault breccias and gouges, and the opening of cracks perpendicular to the movement of the hanging wall. The cracks infilled by cemented breccias are typically oriented perpendicular to the slide surface (Fig. 5a, compare "slide surface" and "clastic dikes") and to the slide direction at each point, and they always appear close to the main slide surface. They are therefore interpreted as clastic dikes associated with motion along the main slide surface.

The characteristics of the deformation associated with the Tazo landslide (the formation of low cohesion fault rocks, fault breccias and gouges) indicate strong, brittle deformation conditions at very high structural levels at depths lower than 4 km (Twiss and Moores 1992). As seen previously, the deformation has affected both the materials belonging to the Lower Old Edifice (pahoehoe flows, sills and dikes) and the rocks of the Basal Complex (gabbros, pyroxenites, submarine volcanic rocks, and dikes), whose different fabrics and mechanical behaviour gave rise to contrasting structures.

In the case of the lava flows, dikes, and sills of the Lower Old Edifice, the generation of fault breccias and granular gouges would essentially have been related to the cataclastic flow (Blenkinsop 2000). In the case of the rocks of the Basal Complex, the deformation associated with the landslide in the footwall is indicated by the formation of an incipient fracture cleavage, marked by the presence of numerous small faults in the damaged zone. It is very possible that the presence of metamorphic minerals (actinolite, chlorite, epidote, albite) arising from the hydrothermal greenschist metamorphism shown by the rocks of the Basal Complex would have conditioned the different pattern of deformation of these rocks, as compared with the unaltered lavas, dikes, and sills of the Lower Old Edifice. The transformation of disaggregated host rocks into assemblages of breccia, and then gouge, records the progressive increase in the total shear strain imposed by the cumulative slip of the landslide. Additionally, the mobilization of the granular gouge that fills small cracks as clastic dikes cutting across the slip plane and intruding the overlying volcanic-breccia deposits (Fig. 6b) suggests the presence of high pore-fluid pressures within the landslide surface (Day 1996). The deformation of the footwall would have been coeval with the landslide process, although it probably lasted for an undetermined period of time prior to the catastrophic event. During that period, the rocks were gradually deformed in a process similar to creep. After the yield strength had been attained, the sudden gravitational collapse of a large portion of the edifice occurred.

The mechanism of gouge formation was probably frictional shearing owing to the emplacement of the overlying cohesive debris flow or debris avalanche. The presence of frictional gouge at the base of volcanic or non-volcanic landslide deposits ("frictionites") or slumps has been reported worldwide. For instance, in the San Andrés fault, on the island of El Hierro (Canary Islands), which is interpreted as having been produced by an aborted sliding (Day et al. 1997), there are cataclasites formed at shallow depths, attributed to large displacements along the fault during a single event. Fine-grained layers at the base of debris-avalanche deposits showing shearing features have been reported for other volcanic locations, such as the debris-avalanche of the Chimborazo sector collapse, in Ecuador, Bernard et al. (2008). Schneider and Fisher (1998) found a zone of strongly foliated gouge at the base of a debris avalanche related to the collapse of the north-western flank of the Cantal Volcano. This foliated gouge overlies a Variscan leucogranite. The gouge fills open cracks in the underlying leucogranite, forming clastic dikes. Those authors concluded that the formation of the gouge and the opening of cracks in the leucogranitic basement were contemporaneous, and that the frictional shearing due to the emplacement of the debris avalanche generated the gouge. On Réunion Island, the lava flows located under the Saint-Gilles breccias that represent debris-avalanche deposits produced by the slide of the western flank of the Piton des Neiges exhibit an intense striation and cataclasis due to the friction and rubbing of the slid mass over the upper surface of the lava flows (Bachèlery et al. 2003). Those authors described the appearance of frictional surfaces at the contacts between the diverse rocky avalanche breccia levels that make up the "Saint Gilles breccias" unit on Réunion Island. They are characterized by shearing bands and fine-grained cataclasites produced by the deceleration affecting the slid

masses when they passed over topographical irregularities (indicated by a change in the slope angle) on the shore of the island. Similar characteristics have been observed in non-volcanic slides. The study of giant submarine landslides has revealed the presence of erosional slide scars, striations on the basal sliding surface, and landslide blocks within a chaotic debris-flow matrix (e.g. Gee et al. 2006). Transitions from rock- and debris-avalanches to distal debris flows have been described in large continental landslides associated with excessive rainfall periods in mountainous areas (Shang et al. 2003). The friction-related gouge recognized at the base of the volcanic breccia above the slip plane of the landslide of Tazo suggests an *en masse* emplacement. Consequently, deposition would have occurred when the debris avalanche or the cohesive debris flow behaved as a rigid sliding mass. Friction probably acted during the last stages of transport, because friction leads to a rapid slowing down and arrest of the debris avalanche or the cohesive debris flow. Before complete arrest of the granular mass, the debris avalanche or the cohesive debris flow would have had to change from a non-turbulent fluidized state into a rigid solid state. This rheological transformation probably occurred very quickly, as suggested by Schneider and Fisher (1998).

The kinematic data reported here provide further information about the sliding process. At many of the points studied, the kinematic criteria point to an ENE-WSW-trending displacement and extension (Figs. 5 and 7). The structures associated with this direction of extension will be referred as Set 1, and include the folds at Point 2 (Fig. 5a), the small faults at Point 4, the folded dikes, faults, and slickenside striations observed on the slide surface at Point 5 (Fig. 7a), and the older striations on the slide surface at Point 6 (Fig. 7b). However, for an explanation of the large-scale geometry of this slide a NNW-SSE collapse would be required (Figs. 2 and 8). In fact, the axis of the curved, concave-upwards sliding surface is NNW-SSE-trending and plunges slightly to the NNW (Fig. 9a). Indeed, some local structures strongly suggest late N-S to NNW-SSE displacements, such as the clastic dikes at Point 2 (Fig. 5a, b), the late faults at Point 4 (Fig. 5c), and the younger striation on the sliding surface at Point 6 (Fig. 7b). These younger structures will be referred to as Set 2. The field data also suggest that both sets of structures developed within a short interval of time from each other. For example, the clastic dikes are almost perpendicular to the axes of the previous folds. Although the structures of Set 2 are usually later than those of Set 1, more complex cross-cut relationships are observed locally, with faults indicating NNW extension displaced by the faults of Set 1 and, again, both generations of structures affected by the faults of Set 2. Rotation of the blocks also produced local features, such as rotated low-angle normal faults, currently with an apparently reverse displacement, and true reverse faults, probably due to stress heterogeneities or to local buttressing effects (Fig. 5c). All these data are coalesced in Fig. 9b and c. The blue and red arrows indicate the old (Set 1) and more recent (Set 2) displacements, respectively. How should this pattern of two, almost normal displacement fields be interpreted, and how should it be reconciled with the evolution of a large volcano flank slide such as the Tazo collapse? A possible analogue can be observed in the tectonic evolution of the island of Stromboli. There, the local extension direction became reoriented in the footwall of the large slide from a regional NW-SE trend towards a radial pattern, perpendicular to the limits of the unbuttressed depression of the sector collapse (Tibaldi 1996). Another factor that would have favoured this extension perpendicular to the slide boundary is the rollover of the upper surface of the spreading block and its substratum. The ENE-WSW extension direction (blue arrows, Fig. 9) and associated faults may have been a response to the large-scale folding of the displaced block. The structures of Set 2 (red arrows in Fig. 9) reflect the large-scale displacement trajectories associated with the collapse. Similar trajectories have been obtained in analogous models of volcanoes spreading above tilted substrata (Wooller et al. 2004) or of flank-collapse in weak-cored volcanoes (Cecchi et al. 2005). Although the large-scale folding and collapse of the hanging wall were essentially contemporaneous processes (actually, the folding process is a result of the displacement of the hanging wall block above its curved basal surface), we believe that most of the deformation related to the folding took place early on during the collapse. A detailed structural analysis of zones similar to the Tazo slide would be necessary to better understand the physical process of the gravitational collapse of large volcanoes.

Interpretation of the deposits filling the amphitheatre formed by the Tazo landslide and their significance in the context of the Canary Islands

The rocks infilling the scar of the Tazo landslide are composed of two successive unconformity-bound units with different textural features, sedimentary structures, and origins.

The sedimentological features of the lower unit, located above the slide surface, suggest that both deposits were formed by a cohesive debris (a matrix-supported deposit of massive character) and by a debris-avalanche (megablocks up to 15 m in size, jigsaw-fit textures). In this sense, the existence of megablocks and jigsaw-fit textures suggests that the lower unit could have been the result of a cohesive debris-flow deposit that was produced by the transformation of the distal portion of a water-saturated debris

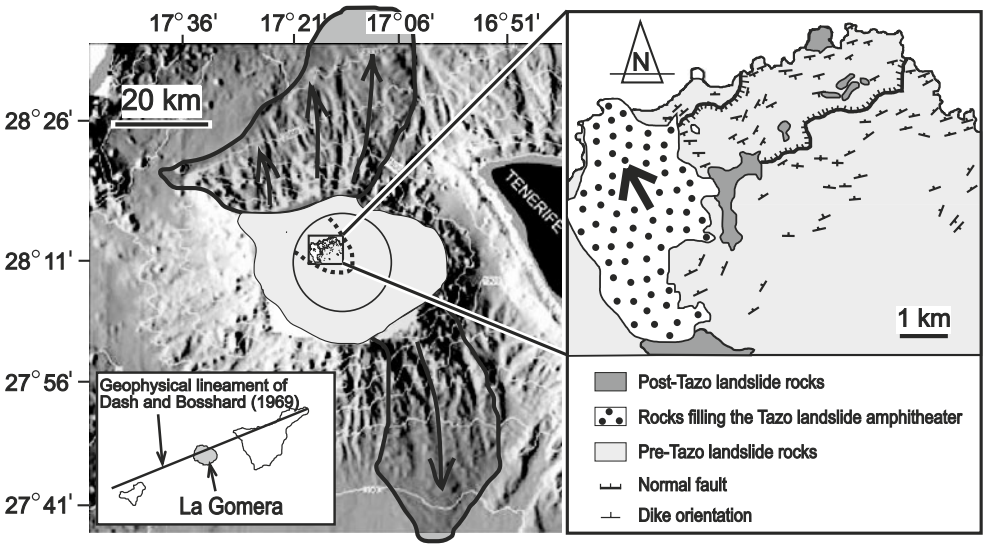

Fig. 8 Sketch showing the possible location, extension, and displacement of the Tazo landslide relative to the Guillama and Montaña de Alcalá faults, the dikes in the Basal Complex, and the geophysical lineament observed by Dash and Bosshard (1969). The estimated dimensions of the Lower Old Edifice were taken from Ancochea et al. (2006). The bathymetric data are from Acosta et al. (2005). The location of the debris-avalanche deposits offshore La Gomera is from Acosta et al. (2005) and the Instituto Español de Oceanografía (2006)

avalanche during its transport (Capra et al. 2002). Alternatively, it is possible that the slide of the flank of the edifice gave rise to a cohesive debris flow directly. In that case, the jigsaw-puzzle texture would have been formed during the initial dilation of the rock at the time of the collapse, and not by the granular collisions during flow, as suggested for Mount St Helens (Glicken 1998). These primary structures may be preserved in the upper portion of the debris-flow deposit. A flank collapse affecting an edifice after an intense hydrothermal alteration (clay-rich), with high water contents (an edifice with an important aquifer), could generate such a cohesive debris flow (Capra and Macías 2000, 2002; Capra et al. 2002), although at Mombacho it did not (Van Wyk de Vries and Francis 1997). The presence of jigsaw-puzzle textures is not exclusive of debris-avalanche deposits; they may also be found in cohesive debris flows coming from the transformation of a debris avalanche (Capra and Macías 2002). The occurrence of an inversely graded layer at the base of the deposit suggests that the flow developed a dilute basal layer, in which the main clast-supporting mechanism was dispersive pressure. This feature is consistent with the hypothesis that mechanical fluidization would have acted as a possible dispersive process for the particles in a large-scale granular flow (Schneider and Fisher 1998).

Concerning the offshore extension of these deposits, Acosta et al. (2005) and the Instituto Español de Oceanografía (2006) have identified several lobes of debris-avalanche deposits located in the north and north-western part of La Gomera, on the ocean floor. The westernmost lobes could correspond to the currently-submerged deposit of the Tazo gravitational landslide (Fig. 8).

The upper unit represents a second stage in the filling of the slide scar, and it contains features attributable both to sediment-charged, high-energy and poorly confined water-laid sheetfloods and hyperconcentrated flows. The scattered cobbles and boulders may represent rock-fall processes (Lirer et al. 2001). This second unit would almost certainly have been formed by the re-sedimentation of the debris-avalanche material formed by the landslide and by the collapse and erosion of the amphitheatre walls.

On the island of Tenerife, in the subsurface of some valleys, such as the Orotava, Güímar or Icod valleys, there are sedimentary deposits buried under hundreds of metres of lava flows that fill ancient paleo-amphitheatres formed by gravitational flank landslides (Bravo 1962; Navarro and Coello 1989; Ancochea et al. 1999). These deposits have been termed "mortalón" (a name given by the people who worked at the many galleries for groundwater exploitation), and consist of chaotic clastic agglomerates composed of rock fragments of all sizes, up to several tons in weight enclosed in a clayey sandy matrix (the "fanglomerado" of Bravo 1962), of laminated clayey-silty deposits of lacustrine origin, and also of conglomerates and breccias originated by debris flow, hyperconcentrated flows, sheetfloods and talus deposits. All these deposits (the so-called "mortalones") have often been interpreted as debris avalanches originated by the gravitational landslides that eroded these valleys (Navarro and Coello 1989). These deposits are sometimes hundreds of metres thick (Bravo 1962; Navarro and Coello 1989; Márquez et al. 2008a, b). However, as shown here most of them are not necessarily debris-avalanche deposits; instead, they could be debris flows, hyperconcentrated flows, sheetfloods, or talus and lacustrine deposits.

The two-episode process of filling the scar formed by the gravitational landslide at Tazo could serve as a model to explain the formation of the above mentioned "mortalón"-type deposits, as has been proposed at other similar landslide amphitheatre infills in the Canary Islands (Playa de La Veta and Cumbre Nueva in La Palma, Colmenero et al. 2008; Teno and Anaga at Tenerife, Walter et al. 2005, Walter and Schmincke 2002) and in other geodynamic

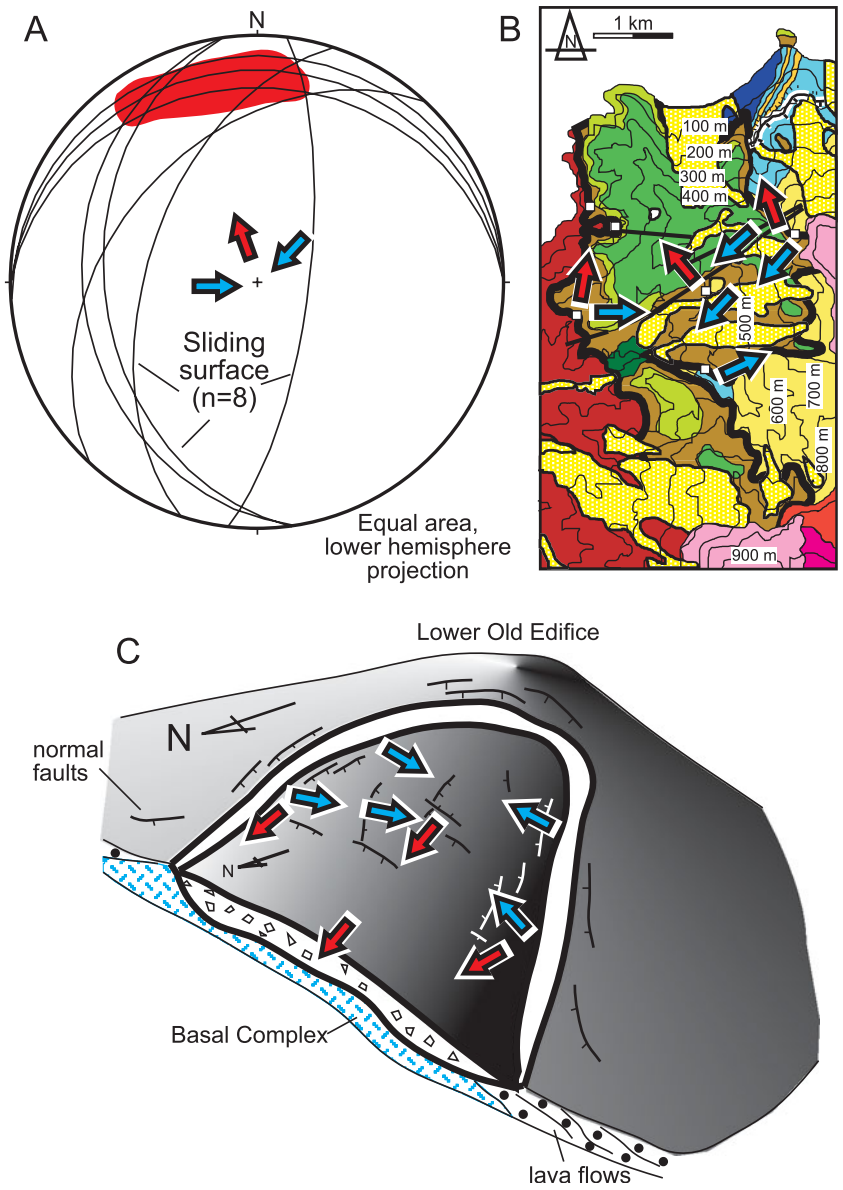

Fig. 9 **a**) Cyclographic projection (equal-area, lower hemisphere) of the sliding surface measured across the entire area studied. The red-shaded area marks the approximate axis of the large-scale, curved sliding surface. The blue and red arrows indicate the sliding direction (or the principal extension axis) at each location for the first and second stages, respectively (see main text for an explanation). **b**) Spatial orientation of the principal extension axes (yellow and red arrows) for the two main stages identified after the structural analysis of the sliding surface, as indicated above. For a legend, see Fig. 2. See main text for an explanation. **c**) Sketch depicting the three-dimensional geometry of the Tazo slide

contexts, such as at the Cantal volcano in France (Reubi and Hernandez 2000; Nehlig et al. 2001; Arnaud et al. 2002) and Etna in Italy (Calvari et al. 1998).

Causes of the slide

Many causes have been proposed to explain the destabilization of large volcanic edifices on Earth, such as those listed by McGuire (1996). These causes are associated with the activity of the volcanoes themselves. They include the intrusion of dikes and sills, the intrusion of cryptodomes or plutonic bodies, the overweight related to the accumulation of volcanic products, phreatic eruptions, vertical collapse related to magma withdrawal in shallow magmatic chambers, seismic activity, and increases in fluid pressure. Factors related to the structure of the edifice itself may also be of relevance, including the presence of hydrothermal alteration zones, olivine cumulates, hydroclastic materials, volcanoclastic, pyroclastic or argillaceous paleosol levels and clayey layers. Finally, the influence of other factors such as gravitational spreading, changes in sea level, or the reactivation of faults in the substratum must also be taken into consideration.

In old landslides it is difficult to know the internal or external causes that triggered the destabilization of the volcanic edifices with any degree of accuracy. Regarding the Old Edifice of La Gomera, the geological data are indicative of a conventional shield volcano (Ancochea et al. 2006). This edifice could have had a diameter of around 22 km (Ancochea et al. 2006). The centre of the original construction would have been situated in the vicinity of Vallehermoso, some 8 km north of the central zone of the

present island (Ancochea et al. 2008). The northern rim of the emergent edifice probably extended for about 5 km offshore from the present northern coastline. This accounts for the shallower and less steep sea floor observed in this area. A volcanic edifice of such dimensions, if slopes dipping from 7° to 10° are assumed, may have reached an altitude of 1,300–1,900 m (Ancochea et al. 2006). This edifice underwent important landslides towards the NW and the NE, which would explain why a large part of its northern flank is currently below sea level (Ancochea et al. 2006).

The slip plane affected very diverse materials with very different mechanical characteristics, ranging from the pahoehoe lavas, sills, and vertical dikes of the Lower Old Edifice, to the submarine volcanic and plutonic rocks of the Basal Complex, intruded by an important dike swarm. The mineralogy of the greenschist facies rocks of the Basal Complex must have diminished their mechanical resistance, facilitating their deformation. Cecchi et al. (2005) have described the flank spreading and collapse of volcanoes with hydrothermally weakened cores, and their predicted deformation field coincides with that corresponding to Set 2 of the structures at the Tazo landslide. Therefore, it is suggested that the Tazo landslide can be considered an example of flank spreading favoured by hydrothermal alteration at the core and base of the edifice, a process so far described for only a few volcanoes (e.g. Casita volcano, Nicaragua, van Wyk de Vries et al. 2000).

The orientation and abundance of the dikes that intruded the rocks of the Basal Complex seem to outline a rift zone in the northern sector of the island that would have been active during the first stages of the formation of the Lower Old Edifice. This rift zone, oriented ENE-WSW, is clearly perpendicular to the slip direction of the Tazo landslide (Fig. 8). On oceanic islands**,** landslides usually occur on the flanks of rift zones (the landslide is oriented perpendicular to a single dominant dike zone) or at the junction of two rifts with different orientations (the sector collapse bisects the angles formed by two intersecting zones of persistent diking (McGuire 1996)). The repeated intrusion of magma into the rift axis could have triggered the Tazo gravitational slide. Additionally, it is necessary to highlight the existence of important ENE-WSW-oriented tectonic features in this northern sector of the island affecting the Basal Complex (Casillas et al. 2008b), such as the normal faults of the Montaña de Alcalá and Guillama (Fig. 1). The ENE-WSW strike of these faults indicates a regional structural trend in the Canary Islands Archipelago. Using seismic and gravimetric methods, Dash and Bosshard (1969) detected a major fracture line that is consistent in orientation and location with those faults and that extends from El Hierro throughout the northern part of La Gomera up to the Teno and Anaga Massifs, both of them in northern Tenerife (Fig. 8). It is very possible that the displacement associated with these regional normal faults could have downthrown the northern part of La Gomera to a considerable extent in a NNW-SSE direction, this being the main cause of the destabilization of this sector of the Lower Old Edifice. Interestingly, the NNW-SSE-directed displacement shown by both regional faults coincides with the collapse direction of the Tazo landslide. This destabilization mechanism was tested experimentally by Vidal and Merle (2000), and later documented by Merle et al. (2006) for the island of Nuku Hiva (Marquesas Archipaelago), considering volcanic edifices of sizes similar to that of the Lower Old Edifice affected by the activity of normal faults. The analogous models of dip-slip faults positioned below the flanks of heterogeneously layered cones (Wooler et al. 2009), which exactly coincide with the location of the Guillama and Montaña de Alcalá faults with respect to the Lower Old Edifice (Figs. 1 and 8), predict the generation of a large-scale instability and collapse perpendicular to the fault strike, in complete agreement with the characteristics of the Tazo landslide.

Conclusions

The Old Edifice of La Gomera underwent a large landslide on its north-western flank. The rocks underlying the slip plane have abundant deformation features. Thus, the lava flows and the dikes of the Lower Old Edifice are folded and intensely crushed, and the slip plane is indicated by the existence of a foliated fault breccia and a foliated granular gouge. Also, where the slip plane affects the rocks of the Basal Complex the dikes are also folded, and the gabbros and pyroxenites are affected by small but numerous faults, which have given rise to the formation of an incipient fracture cleavage. In this case, the slip plane is indicated by the presence of foliated fault breccias and foliated gouges. The slip plane is overlain by a debris avalanche or cohesive debris-flow deposit, the base of which is characterized by the presence of a striated, ultra-fine gouge formed as a consequence of frictional shearing due to the emplacement of the debris avalanche or cohesive debris-flow.

The kinematics of the landslide includes a first stage of extension predominantly perpendicular to the margins of the displaced block, interpreted in the footwall of the sliding mass as being due to a reorientation of the regional deformation field near the border of the newly generated unbuttressed depression. This stage partly coincided in time with the extension parallel to the NNW-directed displacement of the hanging wall block, which generated the dominant deformation field during the last stages of the evolution of the landslide.

This important landslide may be related to the continuous injection of magma, associated with the emplacement of dikes in an ENE-WSW-oriented rift zone, and/or to the displacement associated with the activity of the normal faults of Guillama and Montaña de Alcalá affecting the substratum of the Lower Old Edifice. The low mechanical resistance of the rocks of the Basal Complex, to a large degree affected by a hydrothermal metamorphism under greenschist facies conditions, also facilitated the gravitational collapse of the overlying volcanic edifice.

The filling of the amphitheatre formed by the Tazo landslide occurred in two stages. During the first stage, the materials generated directly by the flank gravitational slide were deposited as a cohesive debris flow or as the product of the flow transformation of the distal portion of a water-saturated debris avalanche. During the second stage, and as a consequence of the re-sedimentation of the former deposits or as a result of the erosion and collapse of the walls of the landslide scars, breccias and conglomerates were deposited by debris flows, hyperconcentrated flows, sheetfloods and talus deposit processes. This model of two filling stages of landslide scars can be extrapolated to other landslides that have occurred in the Canary Islands and to other places in the world, and it provides an alternative to explain the sedimentary deposits found in the subsurface of Tenerife, popularly known as "mortalón".

Acknowledgements Financial support from projects BTE 2003-00569, CGL 2006-00970/BTE and CGL2009-07775 of the Spanish Ministry of Education and Science and the Spanish Ministry of Science and Innovation and 2003/106 of the Canary Islands Regional Government is gratefully acknowledged. The original manuscript benefited from very careful reviews from Jean-Luc Schneider, Benjamin van Wyk de Vries, John Stix and an anonymous reviewer. We are indebted to Nick Skinner for his assistance with the English. The results described in this work were obtained within the framework of the activities of the Research Group "Submarine growth and emergence of the Canary Islands: a geologic study of the Basal Complexes" of the University of La Laguna. We thank Juan Coello Bravo for his comments about the exposures studied in La Gomera.

References

Abdel-Monem A, Walkins ND, Gast P (1971) Potassium-argon ages, volcanic stratigraphy and geomagnetic polarity history of the Canary Islands: Lanzarote, Fuerteventura, Gran Canaria and La Gomera. Am J Sci 271:490–521

Acosta J, Uchupi E, Muñoz A, Herranz P, Palomo C, Ballesteros M, ZEE Working Group (2005) Geologic evolution of the Canarian Islands of Lanzarote, Fuerteventura, Gran Canaria and La Gomera and comparison of landslides at these islands with those at Tenerife, La Palma and El Hierro. Mar Geophys Res 24:1–40

Ancochea E, Huertas MJ, Cantagrel JM, Coello J, Fúster JM, Arnaud N, Ibarrola E (1999) Evolution of the Cañadas edifice and its implications for the origin of the Cañadas Caldera (Tenerife, Canary Islands). J Volcanol Geotherm Res 88:177–1999

Ancochea E, Hernán F, Huertas MJ, Brändle JL, Herrera R (2006) A new chronostratigraphical and evolutionary model for La Gomera: implications for the overall evolution of the Canarian Archipelago. J Volcanol Geotherm Res 157:271–293

Ancochea E, Brändle JL, Huertas MJ, Hernán F, Herrera R (2008) Dike-swarms, key to the reconstruction of major volcanic edifices: the basic dikes of La Gomera (Canary Islands). J Volcanol Geotherm Res 173:207–216

Arnaud N, Leyrit H, Nehlig P, Binet F, Jamet A, Vannier W (2002) Les lahars du flanc nord-ouest du stratovolcan du Cantal. Géol Fr 1:3–13

Bachèlery P, Robineau B, Courteaud M, Savin C (2003) Debris avalanches on the western flank of Piton des Neiges shield volcano (Reunion Island). Bull Soc Géol Fr 174:125–140

Bernard B, van Wyk de Vries B, Barba D, Leyrit H, Robin C, Alcaraz S, Samaniego P (2008) The Chimborazo sector collapse and debris avalanche: deposit characteristics as evidence of emplacement mechanisms. J Volcanol Geotherm Res 176:36–43

Blenkinsop TG (2000) Deformation microstructures and mechanisms in minerals and rocks. Kluwer, Dordrecht

Bravo T (1962) El circo de Las Cañadas y sus dependencias. Bol R Soc Esp Hist Nat Secc Geol 60:93–108

Bravo T (1964) Estudio geológico y petrográfico de la Isla de La Gomera I: estudio geológico. Estud Geol 20:1–21

Calvari S, Tanner LH, Groppelli G (1998) Debris-avalanche deposits of the milo lahar sequence and the opening of the Valle del Bove on Etna volcano (Italy). J Volcanol Geotherm Res 87:193–209

Cantagrel JM, Cendrero A, Fúster JM, Ibarrola E, Jamond C (1984) K-Ar chronology of the volcanic eruption in the Canarian Archipelago: Island of La Gomera. Bull Volcanol 47:597–609

Capra L, Macías JL (2000) Pleistocene cohesive debris fows at Nevado de Toluca Volcano, central Mexico. J Volcanol Geotherm Res 102:149–168

Capra L, Macías JL (2002) The cohesive Naranjo debris-flow deposit (10 km^3): A dam breakout flow derived from the Pleistocene debris-avalanche deposit of Nevado de Colima Volcano (Mexico). J Volcanol Geotherm Res 117:213–235

Capra L, Macías JL, Scott KM, Abrams MD, Garduño-Monroy VH (2002) Debris avalanches and debris flows transformed from collapses in the Trans-Mexican Volcanic Belt, Mexico—behavior, and implications for hazard assessment. J Volcanol Geotherm Res 113:81–110

Casillas R, De la Nuez J, Fernández C, García-Navarro E, Colmenero JR, Martín MC (2008a) La secuencia volcánica submarina del Complejo Basal de La Gomera. Geotemas 10:1273–1276

Casillas R, Fernández C, De la Nuez J, García Navarro E, Colmenero JR, Martín MC (2008b) Deformaciones asociadas al deslizamiento gravitacional de flanco del Edificio Antiguo Inferior en Tazo (La Gomera). Geotemas 10:1269–1272

Cecchi E, van Wyk de Vries B, Lavest JM (2005) Flank spreading and collapse of weak-cored volcanoes. Bull Volcanol 67:72–91

Cendrero A (1971) Estudio geológico y petrológico del Complejo Basal de la Isla de La Gomera (Islas Canarias). Estud Geol 27:3–73

Cladouhos TT (1999) Shape preferred orientations of survivor grains in fault gouge. J Struct Geol 21:419–436

Colmenero JR, de la Nuez J, Casillas R, Castillo C (2008) Caracteres de los conglomerados y brechas epiclásticos de La Palma (Islas Canarias) y su relación con grandes deslizamientos y génesis de la Caldera de Taburiente. Geotemas 10:123–126

Cueto L, Balcells R, Gómez-Saínz JA, Barrera JL, Pineda A, Klein E, Cerrato M, Ruiz MT, Brändle JL (2004a) Mapa y memoria explicativa de la hoja de Hermigüa (1097 III) del Mapa Geológico Nacional. Instituto Geólogico y Minero de España, Madrid, scale 1:25.000, 1 sheet

Cueto L, Gómez-Saínz JA, Barrera JL, Pineda A, Balcells R, Cerrato M, Klein E, Ruiz MT, Brändle JL (2004b) Mapa y memoria explicativa de la hoja de Agulo (1097 IV) del Mapa Geológico Nacional. Instituto Geólogico y Minero de España, Madrid, scale 1:25.000, 1 sheet

Dash BF, Bosshard E (1969) Seismic and gravity investigations around the western Canary Islands. Earth Planet Sci Lett 7:169–177

Day SJ (1996) Hydrothermal pore fluid pressure and the stability of porous, permeable volcanoes. In: McGuire WJ, Jones AP, Neuberg J (eds) Volcano instability on the earth and terrestrial planets. Geol Soc Lond Spec Pub 110:77–93

Day SJ, Carracedo JC, Guillou H (1997) Age and geometry of an aborted rift flank collapse: the San Andres fault system, El Hierro, Canary Islands. Geol Mag 134:523–537

Démeny A, Casillas R, Hegner E, Vennemann TW, Nagy G, Sipos P (2010) Geochemical and H-O-Sr-Nd isotope evidence for magmatic processes and meteoric-water interactions in the Basal Complex of La Gomera, Canary Islands. Mineral Petrol 98:181–195. doi:10.1007/s00710-009-0071-4

Gee MJR, Gawthorpe RL, Friedmann SJ (2006) Triggering and evolution of a giant submarine landslide, offshore Angola, revealed by 3D seismic stratigraphy and geomorphology. J Sed Res 76:9–19

Glicken H (1998) Rockslide-debris avalanche of May 18, 1980, Mount St. Helens Volcano, Washington. Bull Geol Surv Jpn 49:55–106

Herrera R (2008) Volcanoestratigrafía, composición y evolución de los edificios volcánicos subaéreos de La Gomera. PhD thesis, Universidad Complutense de Madrid

Herrera R, Huertas MJ, Ancochea E (2008) Edades ^{40}Ar–^{39}Ar del Complejo Basal de la isla de La Gomera. Geogaceta 44:7–10

Instituto Español de Oceanografía (2006) Mapa Topobatimétrico del Archipiélago Canario. Instituto Español de Oceanografía

Lirer L, Vinci A, Alberico I, Gifuni T, Bellucci F, Petrosino P, Tinterri R (2001) Occurrence of inter-eruption debris flow and hyperconcentrated flood-flow deposits on Vesubio volcano, Italy. Sed Geol 139:151–167

Mardia KV (1972) Statistics of directional data. Academic, London

Márquez A, López I, Herrera R, Martín-Gonzalez F, Izquierdo T, Carreño F (2008a) Spreading and potential instability of Teide Volcano, Canary Islands. Geophys Res Lett 35:L05305. doi:10.1029/2007GL032625

Márquez A, López I, Herrera R, Martín-González F, Izquierdo I, Carreño F (2008b) Reconstrucción geológica tridimensional del basamento del volcán Teide bajo el Valle de Icod y la Caldera de Las Cañadas (Tenerife, Islas Canarias). Geotemas 10:1305–1308

Marrett R, Allmendinger RW (1990) Kinematic analysis of fault-slip data. J Struct Geol 12:973–986

McGuire WJ (1996) Volcano instability: a review of contemporary themes. In: McGuire WJ, Jones AP, Neuberg J (eds) Volcano instability on the earth and terrestrial planets. Geol Soc Lond Spec Pub 110:1–23

Mehl KW, Schmincke H-U (1999) Structure and emplacement of the Pliocene Roque Nublo debris avalanche deposits, Gran Canaria, Spain. J Volcanol Geotherm Res 94:105–134

Merle O, Barde-Cabusson S, Maury R, Legendre C, Guille G, Blais S (2006) Volcano core collapse triggered by regional faulting. J Volcanol Geotherm Res 158:269–280

Miller MG (1996) Ductility in fault gouge from a normal fault system, Death Valley, California: a mechanism for fault-zone strengthening and relevance to paleoseismicity. Geology 24:603–660

Navarro JM, Coello J (1989) Depressions originated by landslide processes in Tenerife. Meeting on Canarian Volcanism, Eur Sci Found, Strasbourg, France

Nehlig P, Leyrit H, Dardon A, Freour G, De Ggoër de Herve A, Huguet D, Thiéblemont D (2001) Repeated growth and catastrophic destruction of the Cantal stratovolcano (France). Bull Soc Géol Fr 172:295–308

Paris R, Guillou H, Carracedo JC, Pérez-Torrado FJ (2005) Volcanic and morphological evolution of La Gomera (Canary Islands), based on new K-Ar ages and magnetic stratigraphy: implications for oceanic island evolution. J Geol Soc Lond 162:501–512

Ramsay JG, Huber MI (1987) The techniques of modern structural geology. Volume 2: folds and fractures. Academic, London

Reubi O, Hernandez J (2000) Volcanic debris avalanche deposits of the upper Maronne valley (Cantal volcano, France): evidence for contrasted formation and transport mechanisms. J Volcanol Geotherm Res 102:271–286

Roa K (2003) Nature and origin of toreva remnants and volcaniclastics from La Palma, Canary Islands. J Volcanol Geotherm Res 125:191–214

Schneider J-L, Fisher RV (1998) Transport and emplacement mechanisms of large volcanic debris avalanches: evidence from the northwest sector of Cantal Volcano. J Volcanol Geotherm Res 83:141–165

Shang Y, Yang Z, Li L, Liu D, Liao Q, Wang Y (2003) A super-large landslide in Tibet in 2000: background, occurrence, disaster, and origin. Geomorphology 54:224–243

Tibaldi A (1996) Mutual influence of dyking and collapses at Stromboli volcano, Italy. In: McGuire WJ, Jones AP, Neuberg J (eds) Volcano instability on the earth and other planets. Geol Soc Lond Spec Pub 110:55–63

Twiss R, Moores E (1992) Structural geology. Freeman, New York

Van Wyk de Vries B, Francis PW (1997) Catastrophic collapse at stratovolcanoes induced by gradual volcano spreading. Nature 387:387–390. doi:10.1038/387387a0

Van Wyk de Vries B, Kerle N, Petley D (2000) A sector collapse forming at Casita volcano, Nicaragua. Geology 28:167–170

Vidal P, Merle O (2000) Reactivation of basement faults beneath volcanoes: a new model of flank collapse. J Volcanol Geotherm Res 99:9–26

Walter TR, Schmincke H-U (2002) Rifting, recurrent landsliding and Miocene structural reorganization on NW-Tenerife (Canary Islands). Int J Earth Sci 91:615–628

Walter TR, Troll VR, Cailleau B, Belousov A, Schmincke HU, Amelung F, Bogaard P (2005) Rift zone reorganization through flank instability in ocean island volcanoes: an example from Tenerife, Canary Islands. Bull Volcanol 67:281–291

Wooler L, van Wyk de Vries B, Cecchi E, Rymer H (2009) Analogue models of the effect of long-term basement fault movement on volcanic edifices. Bull Volcanol 71:1111–1131

Wooller L, van Wyk de Vries B, Murray JB, Rymer H, Meyer S (2004) Volcano spreading controlled by dipping substrata. Geology 32:573–576